Fundamental Limits of Performance in Minimum-Time Motion Control due to Structural Flexibility

Mem. Muroran Inst. Tech., 62(2012) 7~14

特　　集

Fundamental Limits of Performance in Minimum-Time Motion Control due to Structural Flexibility

Boonruk SUCHAITANAWANIT* and Matthew O.T. COLE*

(Received 1 February 2012, Accepted 17 January 2013)

This paper considers the problem of producing time-optimal rest-to-rest motion of a mechanical system subject to limits of actuation effort. Linear dynamic models of a single-mode vibratory structure are considered for two different cases of velocity-limited and force-limited actuation. Minimum-time solutions for rest-to-rest motion with zero residual vibration are obtained by considering geometric constraints for state variables trajectories. This set of equations is reduced and then solved by a root-finding procedure to obtain switching times for the control input signal. The overall speed of motion obtained using the optimal input solution can be considered as a fundamental limit for the achievable performance of a given system. The set of time-optimal solution are therefore presented to show how the speed of motion varies with actuator capacity. These results provide useful information and guidance for matching actuator capacity with flexible structure characteristics of a system under control.

Keywords : Motion control, Flexible structures, Minimum-time motion, Optimal control

1 INTRODUCTION

For mechanical structures under high speed motion, induced vibration due to structural flexibility may need to be considered and accounted for in the actuation scheme. Disk drives[1][2], spacecraft structures[3][4], robots and cranes[5] are well-known examples where this issue comes to bear.

There have been numerous research studies that focus on finding open-loop control solutions for a vibratory mechanical system that give minimum-time motion subject to limits of actuation effort[3][6][7][8]. Time-optimal motions are found to require 'bang-bang' actuation signals that involve multiple switches between two extreme values. For an undamped system (with applied force as the control input) the actuation signal required for rest-to-rest motion is anti-symmetric about the mid-point of the motion interval[3]. Also, a single-mode structure usually requires only three switches of input value during the whole motion[6][7].

The general time-optimal control problem is hard to solve analytically. Various numerical algorithms have been proposed based on application of Pontryagin's minimum principle to the time-optimal Hamiltonian function[3][6][7]. For an undamped single-mode system, an analytical solution can be obtained[3]. Usefully, certain time-optimal motions can also be obtained through a technique known as input shaping where a time-delay filter is applied to a step input signal in order to generate the optimal control input[2][8].

This paper considers two important cases of the time-optimal motion control problem where a geometric analysis of state variable trajectories allows a direct construction of the solution, thereby avoiding a multi-dimensional numerical search. In each section, we first consider a velocity-input system model and then move on to the more complex force-input model. Section 2 formulates the minimum-time control

* Department of Mechanical Engineering, Faculty of Engineering, Chiang Mai, University, Chiang Mai, Thailand, 50200, E-mail: ong-boonruk@hotmail.com

problem and gives necessary conditions for optimality. The considered boundary conditions correspond to a rest-to-rest motion, meaning that the system is initially at rest and the final state is also a rest state involving no residual vibration of the structure. Section 3 outlines the method used to obtain the solution. Experimental results from applying time-optimal solutions on a typical motion control system are given in section 4. In section 5, the theoretical results are analyzed by considering how the achievable time of motion varies with actuator capacity. For these results, the overall speed of motion obtained with the time-optimal solution may be considered as a fundamental limit for achievable performance. It is therefore useful to know the exact manner in which this limit increases with actuator capacity. The final section provides conclusions.

2 PROBLEM FORMULATION

Motion of a flexible structure (Fig. 1) can be described by a linear model of the form:

$$\dot{x}(t) = Ax(t) + Bu(t), \tag{1}$$

where $A = \text{blockdiag}[A_0, A_i]$ and $B = [B_0^T \quad B_i^T]^T$. The sub-matrix A_0 models the rigid-body mode of the system while the sub-matrix A_i models the flexible mode[3][6]. In general there may be many sub-matrices A_i, one for each flexible mode. This study considers only single-mode systems and thus $i = 1$.

A time-optimal problem objective is to find the control input $u(t)$ that drives the system (1) from an initial position $x(0)$ to a desired final position $x(t_f)$ with minimum final time t_f:

$$\min_{u(t)} t_f. \tag{2}$$

The control input must also satisfy the effort limit condition

$$-U \leq u \leq U, \tag{3}$$

For a rest-to-rest motion, the initial point may be chosen as the origin. We also impose that there is zero residual vibration (ZRV) after the final time. The required boundary conditions can be stated as

$$x(0) = [0 \ldots 0]^T, \ x(t_f) = [\Delta x \ 0 \ldots 0]^T, \tag{4}$$

where Δx is the required travel distance. Thus, (1) – (4) form a complete optimization problem.

2.1 Velocity input model

The system (Fig.1) may be considered with $v_A \in [-V, V]$ as the input to be chosen. State variables are selected as

$$x(t) = [x_A \quad x_{BA} \quad v_B].$$

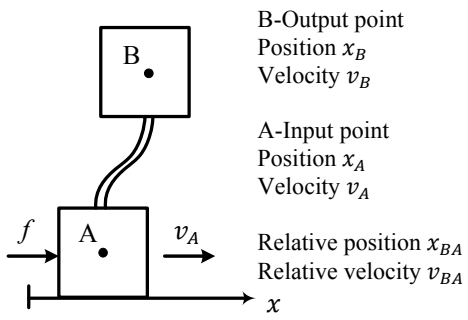

Fig. 1 Rectilinear motion of a flexible structure

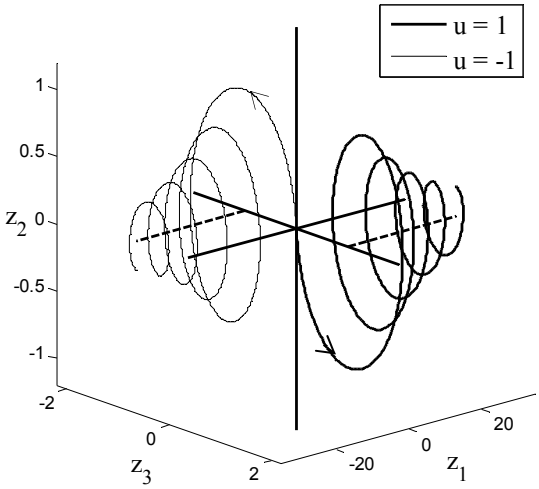

Fig. 2 State trajectories of the velocity input model with damping ($\zeta = 0.05$).

For the rigid body mode, we have

$$A_0 = [0], \ B_0 = [1],$$

and for the vibratory mode we have

$$A_1 = \begin{bmatrix} 0 & 1 \\ -\omega_n^2 & -2\zeta\omega_n \end{bmatrix}, \ B_1 = \begin{bmatrix} -1 \\ -2\zeta\omega_n \end{bmatrix}.$$

Here, ω_n is the natural frequency and ζ the damping ratio. Using the scaled time variable $\tau = \omega_d t$, where $\omega_d = \omega_n\sqrt{1-\zeta^2}$, the model may be transformed to the dimensionless form

$$\dot{z}(\tau) = \begin{bmatrix} 0 & 0 & 0 \\ 0 & -a & 1 \\ 0 & -1 & -a \end{bmatrix} z(\tau) + \begin{bmatrix} 1 \\ -1 \\ a \end{bmatrix} u(\tau), \tag{6}$$

where $u(\tau) \in [-1,1]$ is now the input scaled by the maximum value and $a = \zeta/\sqrt{1-\zeta^2}$. The final condition (4) is also transformed to

$$z(\tau_f) = [\Delta z \ 0 \ldots 0]^T \tag{7}$$

where $\Delta z = \Delta x \omega_d / V$. The model is now independent of the natural frequency but still depends on the

damping ratio through a. Thus, solving the solution of for this model is applicable for the original model with any value of natural frequency.

For a system with damping ($\zeta \neq 0$), state trajectories of (6) are logarithmic spirals with an exponential decay in radius given by $e^{-a\tau}$ (Fig. 2). When $\tau \to \infty$ the trajectory converges to $(z_2, z_3) = (0,1)$ for $u = 1$ and $(z_2, z_3) = (0,-1)$ for $u = -1$. For an undamped system ($\zeta = 0$), trajectories become helical paths around the same pair of axis.

Trajectories shown in Fig. 2 have the origin as the initial point. However the complete set of possible trajectories can be generated by translating, rotating or scaling, with the helix axis as a fixed line.

2.2 Force input model

Mechanical actuation often leads to a system model where force or torque is considered as the input[1-8]. For the model in Fig. 1, we now have the constrained input $f \in [-F, F]$. Compared with the velocity-input case, an additional state variable (usually overall velocity) must be included in the model so that

$$A_0 = \begin{bmatrix} 0 & 1 \\ 0 & 0 \end{bmatrix}, \quad B_0 = \begin{bmatrix} 0 \\ 1 \end{bmatrix}.$$

The model of the vibratory states has the same form as previous and thus, the force input model is

$$\dot{z}(\tau) = \begin{bmatrix} 0 & 1 & 0 & 0 \\ 0 & 0 & 0 & 0 \\ 0 & 0 & -a & 1 \\ 0 & 0 & -1 & -a \end{bmatrix} z(\tau) + \begin{bmatrix} 0 \\ 1 \\ -1 \\ a \end{bmatrix} u(\tau). \qquad (8)$$

The final condition is the same as (7), except in this case $\Delta z = \Delta x \omega_d^2 M/F$ where M is the total mass.

3 SOLVING METHOD

To apply Pontryagin's minimum principle[9][10], we first define the Hamiltonian for $(1) - (4)$ as

$$\mathcal{H} = 1 + \lambda^T(t)\big(Ax(t) + Bu(t)\big), \qquad (9)$$

where $\lambda(t)$ is a co-state vector that satisfies

$$\dot{\lambda}(t) = -\frac{\partial \mathcal{H}}{\partial x} = -A^T\lambda(t). \qquad (10)$$

According to the minimum principle, the necessary conditions along with equations $(1) - (4)$ are

$$u^*(t) = -\mathrm{sgn}\big(B^T\lambda(t)\big) \qquad (11)$$

$$\mathcal{H}(t) = 0, \quad \forall t \in [0, t_f] \qquad (12)$$

where $\mathrm{sgn}(\eta) = 1$ if $\eta > 0$ and $\mathrm{sgn}(\eta) = -1$ if $\eta < 0$. This implies that the optimal control is 'bang-bang' in character[9][10], i.e. $u(t)$ switches between extreme values. It is straightforward to show that the optimal control exists and is unique[9][10]. The essence of the problem here is to establish an initial value of the co-states $\lambda(0)$ such that the corresponding control input given by (11) is consistent with the required boundary conditions (4). If such a $\lambda(0)$ exists then the control input given by (11) is the unique solution to the time-optimal problem.

3.1 Solution for velocity input model

Without damping ($a = 0$), applying $(9) - (12)$ to the model (6), leads to the switching condition

$$u^*(\tau) = \begin{cases} -1 & \lambda_1 > \lambda_2(\tau) \\ 1 & \lambda_1 < \lambda_2(\tau) \end{cases}, \qquad (13)$$

where, according to (10), the co-state λ_1 is constant. To obtain the optimal control from (13), the initial co-state $\lambda(0)$ must be determined. This leads to a binary value problem class which is hard to solve analytically.

By considering the switching condition (13) together with co-state trajectories from equation (10) we can determine that the form of the optimal control is symmetric around the mid-point of the time interval. An example solution is shown in Fig. 3a that also satisfies the ZRV condition. The optimal control is 1 for time T_1 then switches to -1 for time T_2 and finally back to 1 for time T_3. For this undamped case $T_1 = T_3$. The three branches of the state trajectory that make up the optimal motion are shown in Fig. 3b. The trajectory starts at the origin and involves:

I An arc of unit radius about the helix axis $(z_2, z_3) = (0,1)$ through angle T_1 (when $u = 1$).
II An arc about the helix axis $(z_2, z_3) = (0,-1)$ through angle T_2 (when $u = -1$).
III An arc of unit radius about the helix axis $(z_2, z_3) = (0,1)$ through angle T_1 to return to $(z_2, z_3) = (0,0)$ (when $u = 1$).

The final value of z_1 is the distance of motion $\Delta z = 2T_1 - T_2$. The projection of I-III on the z_2-z_3 plane (Fig. 3c) may be considered as rotations of vectors on the complex plane. This leads to the geometric constraint

$$(-e^{jT_1} + 2)e^{jT_2} = (-e^{-jT_1} + 2). \qquad (14)$$

If the distance satisfies $2(n-1)\pi < \Delta z < 2n\pi$, $(n = 2,3, \dots)$, then $n-1$ forward intervals with duration $(2\pi - T_2)$ and n backward intervals with duration T_2 must be included in the motion. When $\Delta z = 2n\pi$, $(n = 1,2,3, \dots)$, then $T_2 = 0$, i.e. no backward interval is required.

For the case with damping ($a \neq 0$), the switching condition is

$$u^*(\tau) = \begin{cases} -1 & \lambda_2(\tau) > \lambda_1 + a\lambda_3(\tau) \\ 1 & \lambda_2(\tau) < \lambda_1 + a\lambda_3(\tau) \end{cases}. \qquad (15)$$

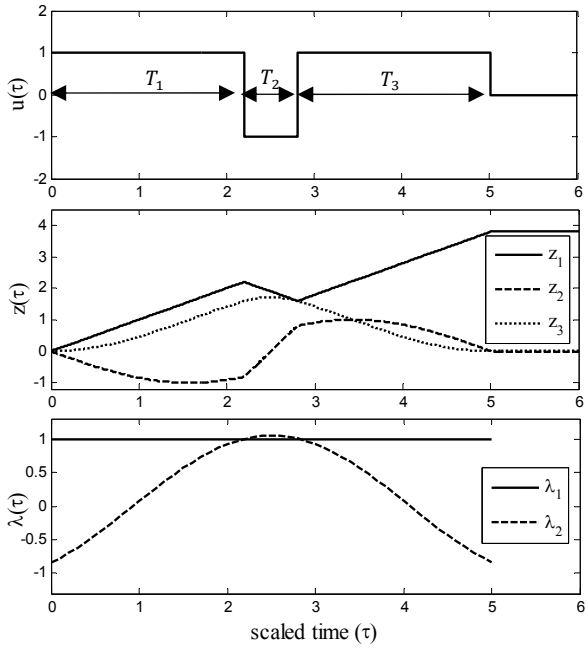

(a) Optimal control input, state, and co-state profile

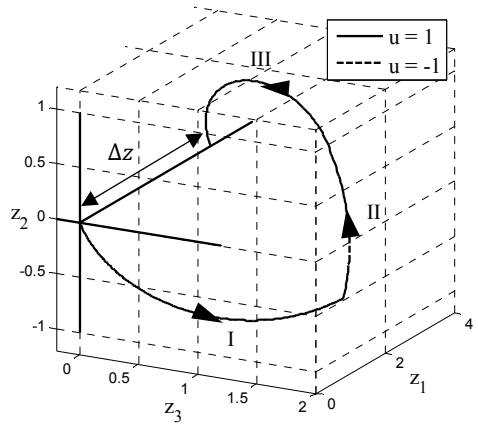

(b) 3D state trajectory

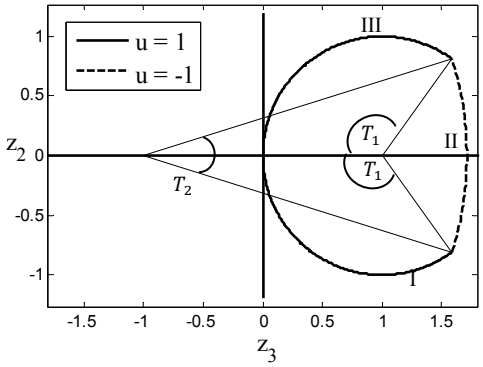

(c) 2D state trajectory with arcs and rotation angles

Fig. 3 Elements of velocity-input solution

A geometric constraint consistent with (15) can be obtained by the same approach as for (14). However, the symmetry requirement does not apply in this case and the resulting condition is

$$\left(-e^{-(a-j)T_1}+2\right)e^{-(a-j)T_2} = \left(-e^{(a-j)T_3}+2\right). \quad (16)$$

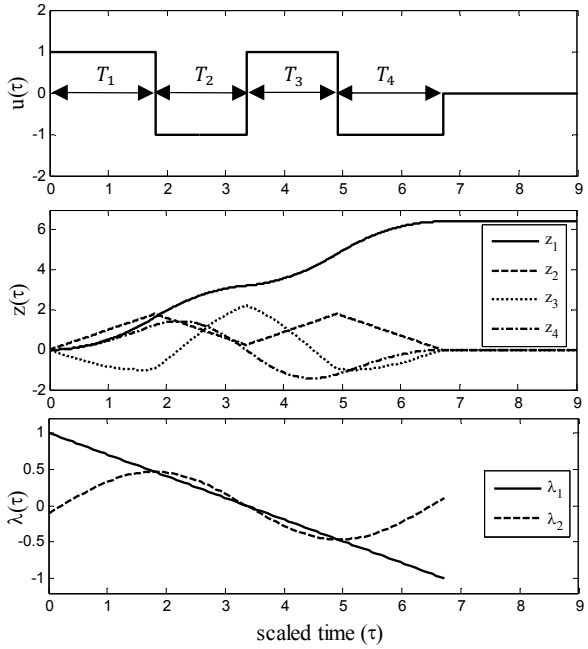

(a) Optimal control input, state, and co-state profile

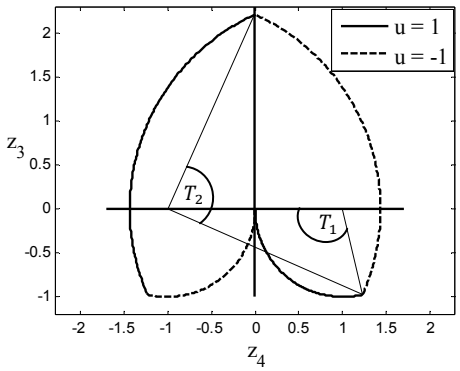

(b) 2D state trajectory

Fig. 4 Elements of force-input solution

Eliminating T_3 from (16) gives

$$\mathrm{Re}(\ln z(T_1,T_2)) + a\,\mathrm{Im}(\ln z(T_1,T_2)) = 0, \quad (17)$$

where $z(T_1,T_2) = \left(-e^{-(a-j)T_1}+2\right)e^{-(a-j)T_2} - 2$. For a given value of T_1, we obtain T_2 from (17) by a root-finding algorithm. T_3 is then computed and the final time obtained as $t_f = T_1 + T_2 + T_3$. After switching times are found, co-state values can also be computed in order to verify the true time-optimality of the solution.

3.2 Solution for force input model

For the undamped case, a switching condition similar to (13) can be derived. According to the co-state trajectory from (10), the optimal solution must be anti-symmetric about the midpoint of the motion[3]. Thus, one additional switch is needed. An additional boundary condition must also be imposed to ensure no residual motion of the rigid body mode (zero final speed). This condition may be expressed

$$T_1 + T_3 = T_2 + T_4 \quad (18)$$

By considering the arcs in Fig. 4b as rotations of complex vectors, the relation between switching times is obtained as the geometric constraint

$$\begin{aligned}&\left(-e^{-(a-j)T_1}+2\right)e^{-(a-j)jT_2}\\&=\left(e^{(a-j)T_4}-2\right)e^{(a-j)T_3}+2.\end{aligned}\qquad(19)$$

For the undamped case ($a=0$), this is equivalent to the solution in [3], but expressed in complex form. Using (18) to eliminate T_4 from equation (19), and then eliminating T_3 gives a similar expression to (17). The value of T_2 may be obtained (again by root-finding) for a given value of T_1 and the remaining switching times computed. In the undamped case, $T_1=T_4$ and $T_2=T_3$ and (19) is more easily reduced.

4 EXPERIMENTS

Optimal solutions for the force-input model have been tested on an experimental system (Fig. 5). The test rig consists of a flexible armature [a] driven by ball screw [b] and dc servo motor [c]. The control input is the torque generated by the dc motor with a current regulating electric drive. Strain gauges [d] are used to measure the deflection at the tip of the armature as a vibratory state of the system. Important parameters of the rig are natural frequency $\omega_n=3.7$ rad/sec and damping ratio $\zeta=0.032$.

Figure 6 compares two example cases of applying: 1) the rigid-body solution and 2) the time-optimal solution for the flexible structure. The distance travelled (6 cm) is the same for the two cases. For the flexible structure solution, the overall motion is seen to be slower than the rigid-body case but residual vibration at the end of motion is almost eliminated.

5 ANALYSIS AND DISCUSSION

It is fairly intuitive that, if velocity is controlled directly, the time-optimal motion for a rigid body involves driving it with maximum velocity until the final position is reached. Thus, the relationship between τ_f and Δz is a straight line (Fig. 7a). With structural flexibility taken into account, an interval with backward motion (negative input velocity) must be introduced. This yields a slower motion than for the rigid-body case, as evident in Fig 7a. However, for an undamped system, there are certain distances for which the total time of motion is equal to the rigid-body case. This occurs when the dimensionless distance is equal to $2\pi, 4\pi, 6\pi,$ ... etc.

With applied force as the input, the fastest way to reach the final position is to accelerate at the maximum rate and then decelerate at the maximum rate after the mid-point of motion. This yields the relation between distance travelled and total time as

$$\tau_f=2\sqrt{\Delta z},\qquad(20)$$

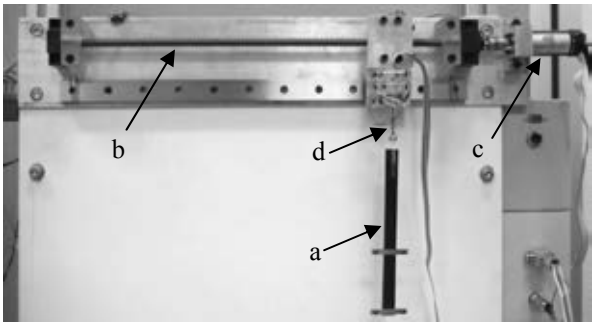

Fig. 5 Experimental rig

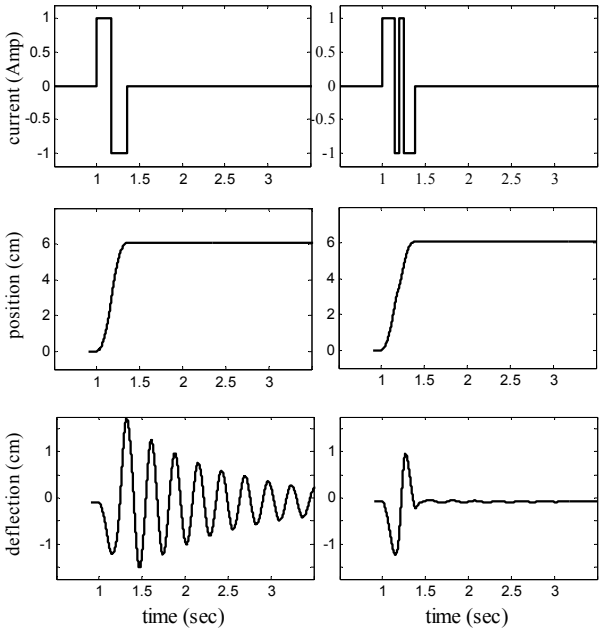

Fig. 6 Experimental results: control input, position, and deflection profiles

With structural flexibility taken into account, additional acceleration and deceleration intervals must be introduced that slow overall motion compared with the rigid-body case (Fig. 7b). Again, for an undamped system there are certain values for the dimensionless distance where no extra switches are needed and the speed of motion matches the rigid-body case, i.e. when $\Delta z=4\pi, 8\pi, 12\pi,$ ...etc.

When damping is present, extra switches are always required. In other words, there is no distance for which the same time of motion as the rigid body case can be achieved.

Each solution obtained corresponds to a pair of values for the dimensionless variables Δz and τ_f. It is usual to interpret the set of solutions as being for fixed maximum input (V or F) and varying over the actual distance traveled Δx. However, for the dimensionless model we have $\Delta z=\Delta x\omega_d/V$ for the velocity input case and $\Delta z=M\Delta x\omega_d^2/F$ for the force input case. Therefore, we may also interpret the solutions as being

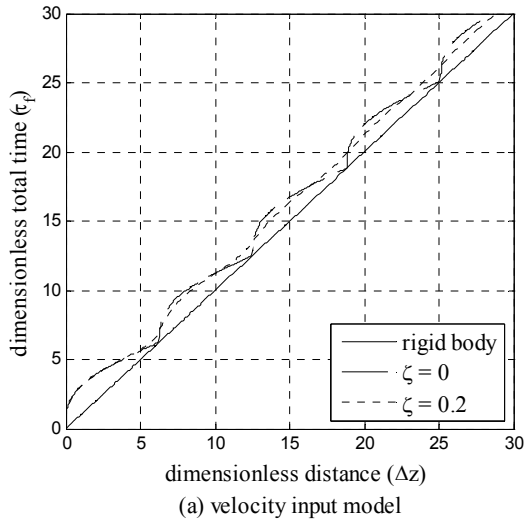

(a) velocity input model

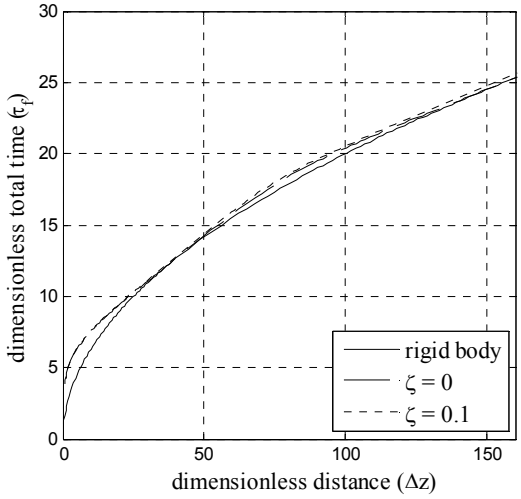

(b) force input model

Fig. 7 Set of time-optimal solutions

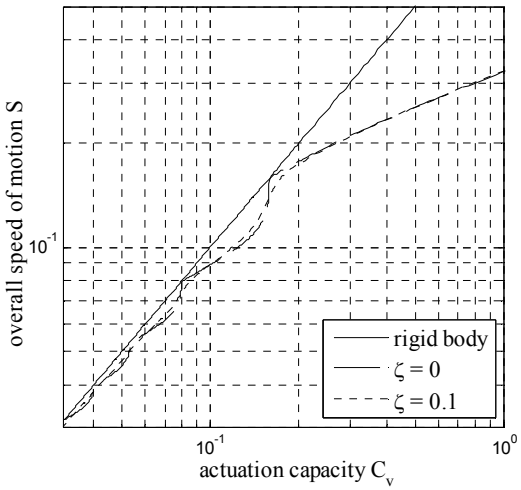

(a) velocity input model

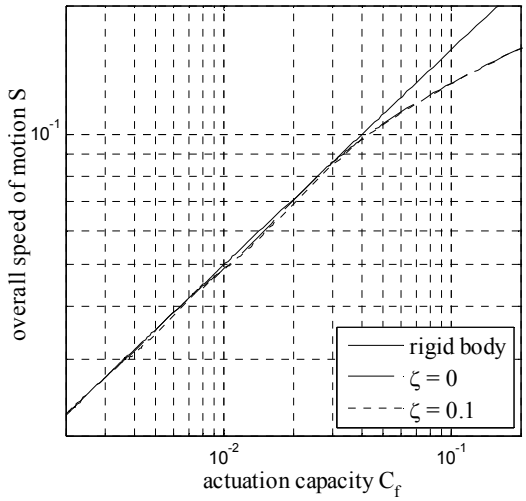

(b) force input model

Fig. 8 Overall speed vs actuation capacity

for fixed Δx and varying over V and F. With this idea, we define the following dimensionless measures of actuation capacity and overall speed of motion:

(a) Relative actuation capacity (velocity input case)

$$C_v := \frac{V}{\Delta x \omega_d} = \frac{1}{\Delta z}$$

(b) Relative actuation capacity (force input case)

$$C_f := \frac{F}{M \Delta x \omega_d^2} = \frac{1}{\Delta z}$$

(c) Overall 'speed' of motion

$$S = 1/\tau_f$$

The value of these parameters may be calculated for each solution. Clearly, the parameter S is a main indicator of the overall performance of the system. The results from plotting S against $C_{v,f}$ are shown in Fig. 8.

For each value of $C_{v,f}$, it is also possible to calculate the corresponding value of S for time-optimal motion of a rigid-body system. For the velocity input case, the input will then have no negative interval and

$$S^{rb} = \frac{V}{\Delta x \omega_d} = C_v.$$

For the force-input case the input has equal positive and negative intervals and so

$$S^{rb} = \frac{1}{2}\left(\frac{F}{M \Delta x \omega_d^2}\right)^{\frac{1}{2}} = \frac{1}{2}\sqrt{C_f}.$$

These two equations define the rigid-body lines seen in Fig. 8 and provide an absolute upper bound on the achievable speed of rest-to-rest motion.

We can see from the results that, when the overall speed of motion is relatively slow, the overall speed for the flexible structure is close to the rigid-body case. However, when the actuation capacity is increased, the average speed can deviate significantly form the rigid-

body line. This effect is most significant when the time interval of motion is of the order of the natural period of vibration of the system (i.e. when $\tau_f \sim 1$) or less.

Also, there is a critical value of the actuation capacity above which speeds close to the rigid-body case can no longer be obtained. For a velocity-input system, this value is given by

$$C_v^{crit} = \frac{V^{crit}}{\Delta x \omega_d} = \frac{1}{2\pi}.$$

For a force input system, the critical value is

$$C_f^{crit} = \frac{F^{crit}}{M\Delta x \omega_d^2} = \frac{1}{4\pi^2}$$

Figure 9 shows speed of motion as a fraction of the rigid-body case versus actuation capacity. The results may be interpreted quantitatively as follows: For the velocity input case, the overall speed of motion is within 78% of the rigid body case if the actuation capacity is below the critical value $(1/2\pi)$. If the actuation capacity is raised beyond this value, speeds close to the rigid-body case can no longer be achieved. For the force input model, the critical actuation capacity is $1/4\pi^2$. In this case, overall speed of motion is within 97% of the rigid-body case if actuation capacity is below the critical value.

This knowledge on limits of performance may be helpful in the design process of actuator selection and sizing. According to the results, high capacity actuation might not give an adequate return, in terms of increased speed of motion, particularly as more powerful actuators tend to be more expensive. The curves in Fig. 8 may be incorporated in an overall design optimization cost function in order to obtain the best solution.

6 CONCLUSIONS

The problem of time-optimal rest-to-rest motion of a single mode flexible structure has been considered. The main contributions of the present work are:

1. The optimal control history is obtained by considering geometric constraints on state variable trajectories.
2. Fundamental characteristics of the solutions, in terms of the relation between actuation effort and overall speed of motion have been presented.

For low overall speed of motion (or relative actuation capacity) the time for motion is close to the case of a rigid body structure. However, if the time of motion is of the order of the natural period of vibration then significant reductions in overall speed are required if zero residual vibration is to be achieved. This fundamental result is explained by the extra intervals with negative input value that are required to cancel elastic vibration of the structure.

Further work aims to extend the results to more general cases where multiple flexible modes and non-linear characteristics of the system are taken into account.

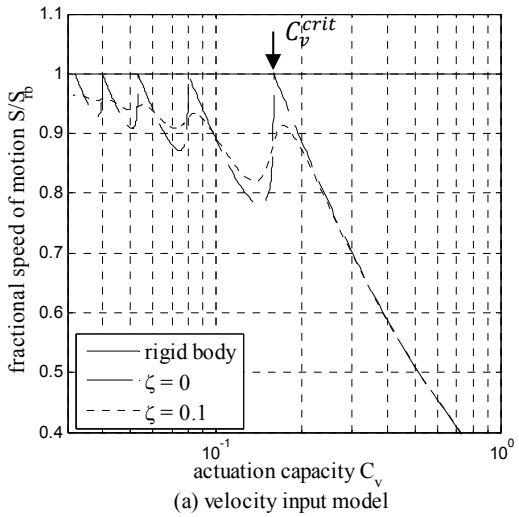

(a) velocity input model

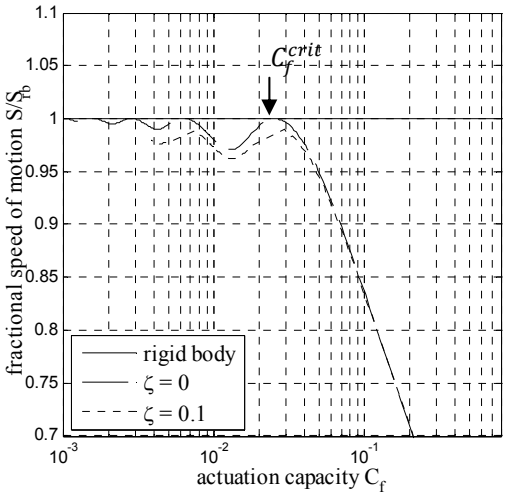

(b) force input model

Fig. 9 Fractional speed vs actuation capacity

ACKNOWLEDGEMENT

This research was partly funded by the Thailand Research Fund (TRF), Royal Golden Jubilee Ph.D. (RJG-Ph.D.) program.

REFERENCES

(1) Weerasooriya, S., Low, T.S., and Huang, Y.H., Adaptive Time Optimal Control of a Disk Drive Actuator, IEEE Transactions on Magnetics, Vol. 30, No.6, (1994), p4224-4226.

(2) La-orpacharapan, C. and Pao, L.Y., Shaped Time-Optimal Control for Disk Drive Systems with Back EMF, Slew Rate Limits, and Different Acceleration and Deceleration Rates, Proceeding of the 2003 American Control Conference, Vol. 6, (2003), p4788-4795.

(3) Singh, G., Kabamba, P. T., and McClamroch, N.H., Planar, Time-Optimal, Rest-to-Rest Slewing Maneuvers of Flexible Spacecraft, Journal of Guidance, Control, and Dynamics, Vol.12, No.1, (1989), p71-81.

(4) Ebrahimi, A., Moosavian, S.A.A, and Mirshams, M., Minimum-Time Optimal Control of Flexible Spacecraft for Rotational Maneuvering, Proceeding of the 2004 IEEE International Conference on Control Applications, Taiwan, Vol. 2, (2004), p961-966.
(5) Auernig, J.W., and Troger, H., Time Optimal Control of Overhead Cranes with Hoisting of the Load, Automatica, Vol. 15, no. 5, (1995), p23-33.
(6) Pao, L. Y. and Frankiln, G.F., Time-Optimal Control of Flexible Structure, Proceeding of the 29th Conference on Decision and Control, Hawaii, Vol.5, (1990), p2580-2581.
(7) Pao, L.Y., Minimum-Time Control Characteristics of Flexible Structures, Journal of Guidance, Control, and Dynamics, Vol.19, No.1, (1996), p123-129.
(8) Singh, T. and Vadali, S.R., Robust Time-Optimal Control: Frequency Domain Approach, Journal of Guidance, Control, and Dynamics, Vol.17, No.2, (1994), p346-353
(9) Kirk, D. E., Optimal Control Theory: An introduction, Dover Publication, (2003).
(10) Lewis, F.L. and Syrmos ,V.L., Optimal Control 2nd edition, John Wiley & Sons, (1995).